Influence of low optical frequencies on actuation dynamics of microelectromechanical systems via Casimir forces

Sedighi Ghozotkhar, Mehdi; Palasantzas, Georgios

Published in:
Journal of Applied Physics

DOI:
10.1063/1.4917081

Influence of low optical frequencies on actuation dynamics of microelectromechanical systems via Casimir forces

Mehdi Sedighi, and George Palasantzas

Citation: Journal of Applied Physics **117**, 144901 (2015); doi: 10.1063/1.4917081
View online: https://doi.org/10.1063/1.4917081
View Table of Contents: http://aip.scitation.org/toc/jap/117/14
Published by the American Institute of Physics

JOURNAL OF APPLIED PHYSICS **117**, 144901 (2015)

Influence of low optical frequencies on actuation dynamics of microelectromechanical systems via Casimir forces

Mehdi Sedighi and George Palasantzas[a)]
Zernike Institute for Advanced Materials, University of Groningen, Nijenborgh 4, 9747 AG Groningen, The Netherlands

(Received 19 January 2015; accepted 27 March 2015; published online 8 April 2015)

The role of the Casimir force on the analysis of microactuators is strongly influenced by the optical properties of interacting materials. Bifurcation and phase portrait analysis were used to compare the sensitivity of actuators when the optical properties at low optical frequencies were modeled using the Drude and Plasma models. Indeed, for metallic systems, which have strong Casimir attraction, the details of the modeling of the low optical frequency regime can be dramatic, leading to predictions of either stable motion or stiction instability. However, this difference is strongly minimized for weakly conductive systems as are the doped insulators making actuation modeling more certain to predict. © *2015 AIP Publishing LLC*. [http://dx.doi.org/10.1063/1.4917081]

I. INTRODUCTION

Modern microelectromechanical system (MEMS) are becoming increasingly important in science and technology revealing simultaneously the significant role of the Casimir force for the design and analysis of microactuators.[1] The Casimir force was predicted by Casimir in 1948 (Ref. 2) when he assumed that two perfectly conducting parallel plates are attracting each other due to perturbation of vacuum fluctuations of the electromagnetic (EM) field.[1–13] Later on Lifshitz and co-workers[3] considered the general case of real dielectric plates by exploiting the fluctuation-dissipation theorem, which relates the dissipative properties of the plates (optical absorption by many microscopic dipoles) and the resulting EM fluctuations. The Lifshitz theory predicts the force between two plates for any material and covers both the short-range (non-retarded) van der Waals and the long-range (retarded) Casimir asymptotic regimes.[1,3] The dependence of the Casimir force on optical properties is an outstanding outcome of the Lifshitz theory[3] because it allows one to tailor the force by suitable choice of interacting materials,[6–16] opening new possibilities for MEMS engineering. These devices have surface areas large enough but gaps small enough for the Casimir force to pull components together leading to permanent adhesion or stiction. This malfunction is very important for the dynamics of MEMS not only as a problem[1,4,14] but also as a means to add more functionalities to MEMS architectures.[1] Moreover, an application of the Casimir oscillator as a separation sensor has been studied in detail in Ref. 17.

So far a sufficiently wide range of materials have been used to measure and calculate the Casimir force using realistic optical properties.[5–13] However, accurate Casimir force measurements have indicated deviations from predictions of dissipation models, e.g., the Drude (D) model having non-zero absorption at frequencies $\omega > 0$ and a singular imaginary part $\sim 1/\omega$ as $\omega \to 0$, used to extrapolate at low optical frequencies where measurements of the optical response is not feasible. On the other hand the Plasma (P) model, which can be thought as a limiting case of the Drude model when dissipation goes to zero (having infinite absorption at the frequency $\omega = 0$ and zero anywhere else) appeared to describe the force data at separations above 160 nm rather well.[13] We have to stress that though the Plasma model does not have strong physical background, it shows interesting behavior and the Casimir force calculation has better agreement with experiment than the Drude model.

Therefore, it becomes an important issue to consider this possibility on actuation dynamics for different materials with significant absorption in the far infrared range due to charge carriers. This discrepancy could possibly be a signature of either an inconsistency in the Lifshitz theory or a contribution of electrostatic surface potential effects[14] or other unknown effect. Independent of the actual reason, this is a fact that has still to be taking into account in modeling of MEMS actuation dynamics.

II. CASIMIR FORCE THEORY AND MATERIAL OPTICAL PROPERTIES

The materials considered here include metallic Au films, which are good conductors and their optical properties have been measured in a wide range of frequencies.[11] Gold is widely used for Casimir force measurements. Finally, as a poor conductor, we consider a wide band gap material, which is the insulating silicon carbide (SiC) but becomes conductive due to nitrogen doping. This material has a prominent phonon-polariton peak followed by a Drude tail at infrared frequencies (see Ref. 16 for measurements and a description of its optical properties). Both type of materials were optically characterized with the same equipment (J. A. Woollam Co., Inc. ellipsometers VUV-VASE (0.5–9.34 eV) and IR-VASE (0.03–0.5 eV)). For clarity, the imaginary parts of Au and SiC are shown in Fig. 1.

Since as a model MEMS device we will consider a sphere-plate geometry system to avoid parallelism problems

[a)]Author to whom correspondence should be addressed. Electronic mail: g.palasantzas@rug.nl.

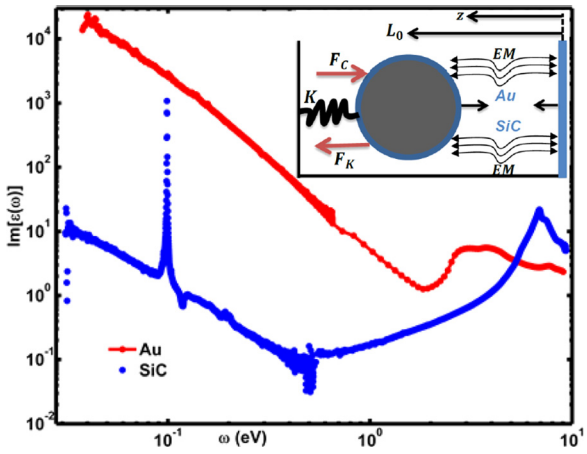

FIG. 1. Imaginary part $\varepsilon''(\omega)$ of the frequency dependent dielectric function measured by ellipsometry for Au and conductive SiC. The inset shows the model sphere-plate geometry device.

(inset Fig. 1), prior to modeling of actuation dynamics we will describe briefly the related Casimir force theory. Within the proximity force approximation (PFA), the Casimir force for separation $z \ll R$, with R the sphere radius, is given by

$$F^{ps}(z) = \frac{\hbar c R}{16\pi z^3}\sum_{\nu}\int_0^1 dt\int_0^{\infty} dx x^2 \ln\left(1 - r_1^{\nu} r_2^{\nu} e^{-x}\right). \quad (1)$$

Equation (1) applies for zero temperature $T = 0$ calculations or for short separations ($z < 300\,nm$) at room temperature since thermal fluctuations have negligible contribution due to the large thermal wavelength $\lambda_T = \hbar c/KT$ ($= 7.6\,\mu m$ at $T = 300\,K$) with $\hbar$ is the Planck constant and c is the speed of light. The integration variables are defined as $x = 2k_0 z$, $tx = \zeta/\zeta_{ch}$, and $\zeta_{ch} = c/2z$. The indices $\nu = s$ and p denote the two polarizations (TE/TM modes), and $r_{1,2}^{\nu}$ are the Fresnel reflection coefficients for body 1 and 2. The latter are defined as $r_i^s = (1 - \sqrt{1 + t^2(\varepsilon_i(i\zeta) - 1)})/(1 + \sqrt{1 + t^2(\varepsilon_i(i\zeta) - 1)})$, and $r_i^p = (\varepsilon_i - \sqrt{1 + t^2(\varepsilon_i(i\zeta) - 1)})/(\varepsilon_i + \sqrt{1 + t^2(\varepsilon_i(i\zeta) - 1)})$. The wave numbers perpendicular to the plates are in the i-th material $k_i = \sqrt{\varepsilon_i(i\zeta)(\zeta^2/c^2) + q^2}$ and in vacuum (or air) $k_0 = \sqrt{(\zeta^2/c^2) + q^2}$ with q the wave number along the plates. Finally, the dielectric function at imaginary frequencies $\varepsilon(i\zeta)$ is given $\varepsilon(i\zeta) = 1 + (2/\pi)\int_0^{\infty} d\omega[(\omega\varepsilon''(\omega))/(\omega^2 + \zeta^2)]$.

Since the experimental data for the imaginary part $\varepsilon''(\omega)$ of the dielectric function $\varepsilon(\omega)$ covers only a limited optical frequency range $\omega_1 (= 0.03\,eV) < \omega < \omega_2 (= 8.9\,eV)$ (Fig. 1). For conductive materials that show absorption due to charge carriers in the infrared range, the Drude model $\varepsilon(\omega)_D = \varepsilon_o - \{\omega_p^2/\omega(\omega + i\omega_\tau)\}$ is often used in extrapolating for $0 < \omega < \omega_1 (= 0.03\,eV)$ with $\varepsilon''(\omega) = \{\omega_p^2\omega_\tau/\omega(\omega^2 + \omega_\tau^2)\}$ (note that $\varepsilon''(\omega) \sim 1/\omega$ as $\omega \to 0$). ω_p is the Plasma frequency, ω_τ is the relaxation frequency, and the ratio $\omega_p{}^2/\omega_\tau$ is indicative of the material static conductivity ($\omega \to 0$). For high optical frequencies, $\omega > \omega_2$, which plays negligible role unless very short separations ($<10\,nm$) are concerned for force calculations, the extrapolation takes place with an inverse power law as $\varepsilon''(\omega) = A/\omega^3$.[16] Therefore, the Drude model yields[16]

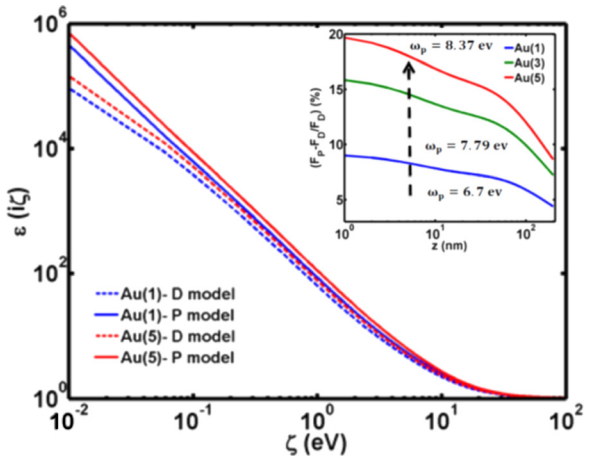

FIG. 2. Calculations of $\varepsilon(i\zeta)$ for Au for the samples 1 and 5 from Ref. 11 using the D-P models. The inset shows Casimir force contrast between D-P models vs. separation for the differently prepared Au samples 1-3-5 in Ref. 11.

$$\varepsilon(i\zeta)_D = 1 + \frac{2}{\pi}\int_{\omega_1}^{\omega_2}\frac{\omega\varepsilon''_{exp}(\omega)}{\omega^2 + \zeta^2}d\omega + \Delta_{L,D}\varepsilon(i\zeta) + \Delta_H\varepsilon(i\zeta), \quad (2)$$

with $\Delta_H\varepsilon(i\zeta) = 2\omega_2^3\varepsilon''(\omega_2)/\pi\zeta^2[1/\omega_2 - ([\pi/2 - \arctan(\omega_2/\zeta)]/\zeta)]$ and $\Delta_{L,D}\varepsilon(i\zeta) = [2\omega_p^2\omega_\tau/\pi(\zeta^2 - \omega_\tau^2)][(\arctan(\omega_1/\omega_\tau)/\omega_\tau) - (\arctan(\omega_1/\zeta)/\zeta)]$.[16] If instead one uses the Plasma model at low optical frequencies $\omega < \omega_1$, then $\Delta_{L,D}\varepsilon(i\zeta)$ in Eq. (2) has to be replaced by $\Delta_L\varepsilon(i\zeta)_p = 1 + \omega_p^2/\zeta^2$ yielding

$$\varepsilon(i\zeta)_P = 1 + \frac{\omega_p^2}{\zeta^2} + \frac{2}{\pi}\int_{\omega_1}^{\omega_2}\frac{\omega\varepsilon''_{exp}(\omega)}{\omega^2 + \zeta^2}d\omega + \Delta_H\varepsilon(i\zeta). \quad (3)$$

The difference between the D-P models for Au films from Ref. 11 is shown in Fig. 2. Figure 2 inset also shows that with decreasing surface separation the force difference between the D-P models increases, and it is sensitive to the actual preparation conditions of the interacting materials with different effective Plasma frequencies ω_p.[11] With increasing ω_p (Ref. 11) the relative force difference between D-P models is ~9–20% as can be seen in Fig. 2. However, for less conductive materials, e.g., the conductive SiC,[16] the differences between the D-P models significantly diminishes as can be seen in Fig. 3.

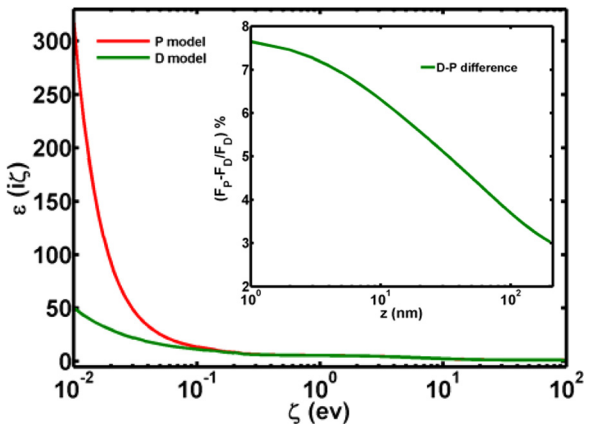

FIG. 3. Calculations of $\varepsilon(i\zeta)$ for SiC (Ref. 16) using both the Drude and Plasma models. The inset shows the relative force difference between the D-P models for SiC.

III. RESULTS ON ACTUATION DYNAMICS OF MEMS

Furthermore, for the study of MEMS actuation dynamics, we consider the model system of a sphere-plate as it is shown in the inset of Fig. 1, which is also common in Casimir force measurement by AFM and MEMS.[8–12] The system components are assumed to be coated with a thick coating (typical thickness ≥ 100 nm) of SiC or Au. The equation of motion, assuming an initial impulse to trigger continuous actuation (with L_0 the separation where the spring is not stretched), has the form[15,16,18–21]

$$M\frac{d^2z}{dt^2}+\left(\frac{M\omega}{Q}\right)\left(\frac{dz}{dt}\right)=-K(L_0-z)+F^{ps}(z). \quad (4)$$

The Casimir force $F^{ps}(z)$ is opposing the elastic restoring elastic force $F_K(z)=-K(L_0-z)$ with K a spring constant. M is the mass of the sphere, and $(M\omega/Q)(dz/dt)$ is the intrinsic energy dissipation. As a starting point, we consider MEMS with high quality factor $Q\geq 10^4$ (Refs. 22 and 23) so that we can neglect dissipation effects, and the frequency ω is assumed to be that of dynamic mode AFM cantilevers and MEMS (typically $\omega=300$ kHz),[23] and an $L_0=200$ nm. In all cases, we will also consider flat surfaces because nanoscale roughness gives significant contributions at low surface separations.[24] Because atomic force microscopy (AFM) analysis indicated almost flat SiC surfaces, with a root-mean-square (rms) surface roughness $w\sim 0.12$ nm (see Fig. B1 in supplemental material of Ref. 16), the influence of roughness was omitted in the present study since our actuation analysis is well above 50 nm surface separations (so that $z\gg w$).

To proceed further we introduce a bifurcation parameter $\lambda=F^{ps}_{SiC}(L_0)/KL_0$,[17–20] which is the ratio of the minimum Casimir force $F^{ps}_{SiC}(L_0)$ (calculated for the SiC using the Drude model) to the maximum elastic force KL_0. In this manner, we can compare the force influence for different materials and dissipation models. If we set the total force in Eq. (4) equal to zero, $F_T=-K(L_0-z^*)+F^{ps}(z^*)=0$, then we can calculate the locus of equilibrium points z^* (Refs. 18–21) via the expression

$$\lambda=(F^{ps}_{SiC}(L_0)/F^{ps}(z^*))(1-z^*/L_0). \quad (5)$$

Since the condition $dF_T/dz^*=K+dF_C/dz^*=0$ (Refs. 18–21) is also satisfied, Eq. (5) gives the critical equilibrium (stationary) points. Figure 4 shows the sensitivity of the parameter λ for Au and SiC using the D-P models. As Fig. 4 shows, if the spring constant is strong enough so that $\lambda<\lambda_{max}\,(=\lambda(z^*_{max}))$, since $\lambda\sim 1/K$, then they exist two equilibrium points. The equilibrium point closest to L_o is a stable center around which periodic solutions exist, while the other closer to the plate is an unstable point around which motion will lead to stiction on the plate due to the stronger Casimir force. The locus of points for $z^*>z^*_{max}$ corresponds to stable actuation.

For lower spring constants K so that $\lambda\geq\lambda_{max}$, then, for example, for the Plasma model for Au, the motion is only unstable favoring stiction on the plate, while there are still two equilibrium points if the Drude model is used. The same applies for the SiC-SiC system since the intercept gives two

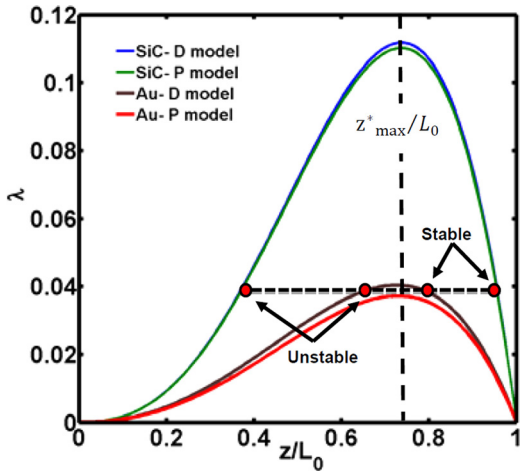

FIG. 4. Bifurcation diagrams for Au-Au and SiC-SiC systems using the D-P models for the Casimir force calculations and $R=10\,\mu$m.

equilibrium points. Since the Casimir force using the Plasma model is stronger, the bifurcation diagrams confirm the fact that the Plasma model predicts more likely unstable motion towards stiction, while the weaker force for the Drude model can lead to stable motion (for both the Au-Au and the SiC-SiC systems in Fig. 4). From Fig. 4, we can also infer that the SiC-SiC system has a much wider range of stable operation with respect to Au-Au, and the MEMS is significantly less sensitive to details of how we extrapolate at low frequencies. If one considers the presence of an additional electrostatic force the physics of the system with respect to its stability will remain similar since the only difference is that the distance between the center and saddle point is smaller.[24]

The system dynamics via the solution of the equation of motion can be described with the so-called phase portraits,[25] which are plots of the velocity dz/dt of the actuating element versus its displacement z. Phase portraits are presented in Fig. 5 using the D-P models. Closed orbits correspond to periodic movement around a stable equilibrium point indicating that the elastic force is strong enough to counterbalance the Casimir force. From these plots, it becomes clear that by only changing the model for the extrapolations at low

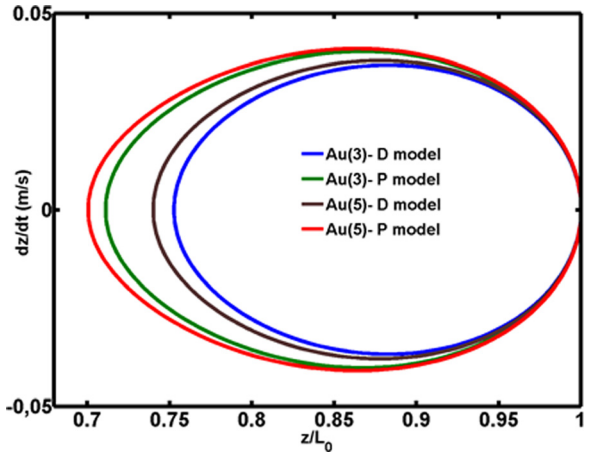

FIG. 5. Phase portraits when the plate is coated with two different Au films (3 and 5) from Ref. 11 for both the D-P models. The spring constant is $K=0.00015$ N/m and $R=10\,\mu$m.

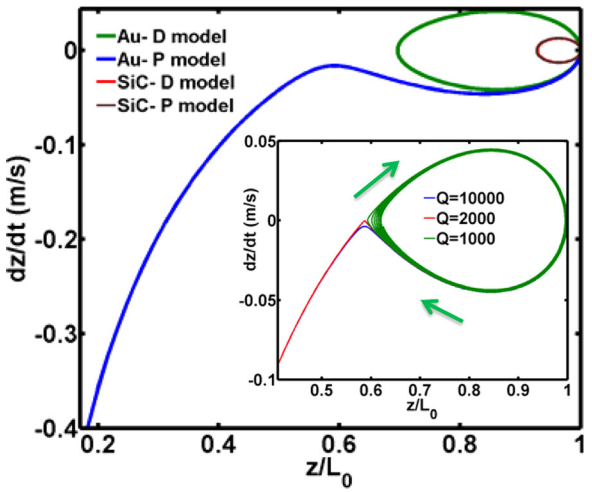

FIG. 6. Phase portrait dz/dt vs. z for different materials for the sphere and plate. Closed orbits show stable motion, while an open orbit is the sign of unstable motion towards stiction on the plate. The inset shows the influence of dissipation with different Q factors on actuation dynamics using the Plasma model for Au. The spring constant is $K = 0.00010\,N/m$ and $R = 10\,\mu m$.

frequencies the domain of system movement is significantly reduced and therefore the system stability is increased. The difference between the two models is notably increasing for the part of the orbit that comes close to the plate since the Casimir force is there strongest. In addition, Fig. 6 shows more details of how a system can transit progressively from stable motion into stiction for the D-P models. If we compare Au-Au and SiC-SiC, then for the latter the actuating component remains safely far from the unstable region and the system experiences only stable movement.

If we pay attention to details around the unstable regime with respect to the D-P model predictions then it becomes evident that for a system with strong Casimir attraction (e.g., Au-Au) the details of the modeling of the low optical frequency regime as $\omega \to 0$ can predict either stable motion (D-model) or stiction dynamics (P-model) at nanoscale separations. However, such a discrepancy is minimized for less conductive systems as the plots for SiC in Fig. 6 clearly shows. Finally, we must point out that although the stronger Casimir force obtained via the Plasma model predicts stiction under conditions of low dissipation ($Q \gg 1$), the introduction of dissipation (decreasing Q factor) can strongly alter the nature of the instability as the inset in Fig. 6 indicates for the Au-Au system. Indeed, as the system quality factor Q decreases by an order of magnitude (e.g., by surface pattering of the resonator),[24] then the stiction instability turns into the more stable dissipative motion towards equilibrium since the work performed on the actuating component by the Casimir force can no longer overcome dissipative losses.

IV. CONCLUSIONS

In conclusion, the dependence of the Casimir force on the frequency dependent dielectric function of interacting materials makes feasible to tailor the actuation dynamics of microactuators. Bifurcation and phase portrait analysis was used to compare the sensitivity of actuators when the optical properties at low frequencies are modeled using both the D-P models. It becomes evident that for a system with strong Casimir attraction (metallic systems, e.g., Au-Au), the details of the modeling of the low optical frequency regime can predict either stable motion or stiction dynamics at nanoscale separations. However, such a difference is strongly minimized for less conductive systems as they are the doped insulators (e.g., conductive SiC) making actuation modeling more certain to predict.

ACKNOWLEDGMENTS

We would like to acknowledge useful discussions with V. B. Svetovoy, W. H. Broer, and support from the Zernike Institute of Advanced Materials, University of Groningen, The Netherlands.

[1]A. W. Rodriguez, F. Capasso, and S. G. Johnson, Nat. Photonics **5**, 211 (2011); P. Ball, Nature (London) **447**, 772 (2007).
[2]H. B. G. Casimir, Proc. K. Ned. Akad. Wet. **51**, 793 (1948).
[3]E. M. Lifshitz, Sov. Phys. JETP **2**, 73 (1956); I. E. Dzyaloshinskii, E. M. Lifshitz, and L. P. Pitaevskii, Sov. Phys. Usp. **4**, 153 (1961).
[4]S. K. Lamoreaux, Phys. Rev. Lett. **78**, 5 (1997); S. K. Lamoreaux, Rep. Prog. Phys. **68**, 201 (2005); H. B. Chan *et al.*, Phys. Rev. Lett. **87**, 211801 (2001); Science **291**, 1941 (2001); Phys. Rev. D **75**, 077101 (2007).
[5]D. Iannuzzi, M. Lisanti, and F. Capasso, PNAS **101**, 4019 (2004).
[6]F. Chen, G. L. Klimchitskaya, V. M. Mostepanenko, and U. Mohideen, Opt. Express **15**, 4823 (2007); G. Torricelli, I. Pirozhenko, S. Thornton, A. Lambrecht, and C. Binns, Europhys. Lett. **93**, 51001 (2011).
[7]S. de Man, K. Heeck, R. J. Wijngaarden, and D. Iannuzzi, Phys. Rev. Lett. **103**, 040402 (2009).
[8]G. Torricelli, P. J. van Zwol, O. Shpak, C. Binns, G. Palasantzas, B. J. Kooi, V. B. Svetovoy, and M. Wuttig, Phys. Rev. A **82**, 010101 (R) (2010).
[9]G. Torricelli, P. J. van Zwol, O. Shpak, G. Palasantzas, V. B. Svetovoy, C. Binns, B. J. Kooi, P. Jost, and M. Wuttig, Adv. Funct. Mater. **22**, 3729 (2012).
[10]C.-C. Chang, A. A. Banishev, G. L. Klimchitskaya, V. M. Mostepanenko, and U. Mohideen, Phys. Rev. Lett. **107**, 090403 (2011).
[11]V. B. Svetovoy, P. J. van Zwol, G. Palasantzas, and J. Th. M. De Hosson, Phys. Rev. B **77**, 035439 (2008).
[12]G. Palasantzas, V. B. Svetovoy, and P. J. van Zwol, Int. J. Mod. Phys. B **24**, 6013 (2010).
[13]R. S. Decca, D. Lopez, E. Fischbach, G. L. Klimchitskaya, D. E. Krause, and V. M. Mostepanenko, Ann. Phys. **318**, 37 (2005); C.-C. Chang, A. A. Banishev, R. Castillo-Garza, G. L. Klimchitskaya, V. M. Mostepanenko, and U. Mohideen, Phys. Rev. B **85**, 165443 (2012).
[14]R. O. Behunin, D. A. R. Dalvit, R. S. Decca, C. Genet, I. W. Jung, A. Lambrecht, A. Liscio, D. Lopez, S. Reynaud, G. Schnoering, G. Voisin, and Y. Zeng, Phys. Rev. A **90**, 062115 (2014); R. O. Behunin *et al.*, Phys. Rev. A **85**, 012504 (2012); **86**, 052509 (2012); J. L. Garrett, D. Somers, and J. N. Munday, Special issue Casimir Forces: J. Phys. Cond. Matt. (2015), available at http://iopscience.iop.org/0953-8984/page/Forthcoming%20articles#Special_isCasimir_Fo.
[15]M. Sedighi, V. B. Svetovoy, W. H. Broer, and G. Palasantzas, "Influence of materials optical response on actuation dynamics by Casimir forces," J. Phys. Cond. Matter. (unpublished); available at http://iopscience.iop.org/0953-8984/page/Forthcoming%20articles#Special_isCasimir_Fo.
[16]M. Sedighi, V. B. Svetovoy, W. H. Broer, and G. Palasantzas, Phys. Rev. B **89**, 195440 (2014). For roughness characteristics of SiC surfaces see also the supplemental material (Fig. B1).
[17]S. Cui and Y. C. Soh, J. Microelectromech. Syst. **19**(5), 1153 (2010).
[18]M. Sedighi, W. H. Broer, G. Palasantzas, and B. J. Kooi, Phys. Rev. B **88**, 165423 (2013).
[19]M. Sedighi and G. Palasantzas, Appl. Phys. Lett. **104**, 074108 (2014).
[20]R. Esquivel-Sirvent, L. Reyes, and J. Bárcenas, New J. Phys. **8**, 241 (2006).
[21]R. Esquivel-Sirvent, M. A. Palomino-Ovando, and G. H. Cocoletzi, Appl. Phys. Lett. **95**, 051909 (2009).

[22]R. Garcıa and R. Perez, Surf. Sci. Rep. **47**, 197 (2002); M. Li, H. X. Tang, and M. L. Roukes, Nature Nanotechnol. **2**, 114 (2007); H. J. Mamin and D. Rugar, Appl. Phys. Lett. **79**, 3358 (2001); D. Rugar, R. Budakian, H. J. Mamin, and B. W. Chui, Nature **430**, 329 (2004).
[23]O. Ergincan, G. Palasantzas, and B. J. Kooi, Phys. Rev. B **85**, 205420 (2012).
[24]W. Broer, G. Palasantzas, J. Knoester, and V. B. Svetovoy, Phys. Rev. B **87**, 125413 (2013).
[25]M. W. Hirsch, S. Smale, and R. L. Devaney, *Differential Equations, Dynamical Systems, and an Introduction to Chaos* (Elsevier Academic Press, San Diego, CA, 2004).